Study of nano bioactive glass for use as bone biomaterial comparison with micro bioactive glass behaviour

IOP Conf. Series: Materials Science and Engineering **628** (2019) 012005 doi:10.1088/1757-899X/628/1/012005

Study of nano bioactive glass for use as bone biomaterial comparison with micro bioactive glass behaviour

N Rocton, H Oudadesse, S Mosbahi, L Bunetel, P Pellen-Mussi and B Lefeuvre

University Rennes, CNRS, ISCR-UMR 6226, F-35000, Rennes, France

Corresponding author's e-mail: hassane.oudadesse@univ-rennes1.fr

Abstract. This research is based on the study of bioactivity kinetic in function of the glass particles size. Bioactive glasses have been elaborated in the ternary system SiO2-CaO-P2O5. Nano bioactive glass and micro bioactive glass have been synthesized by using two different processes. They are destined for use as bone biomaterials. The comparison was focused on the kinetic of the development of a calcium phosphate layer on their surfaces after immersion in a Simulated Body Fluid (SBF). The first bioactive glass BG is a melting-made glass with a particles size of about 60 µm. The second bioactive glass NBG is a sol-gel made glass through an emulsion system of synthesized particles of about 110 nm. The growing of the calcium phosphate layer at the surface of the glasses has been followed using several physicochemical techniques. Obtained results show the development of a calcium phosphate layer similar to carbonated hydroxyapatite. It crystallises in a hexagonal system with an P63/m space group. While melting-made glass needs 14 days to develop carbonated hydroxyapatite like crystal, sol-gel needs only 3 days to develop similar crystals. This difference offers wide opportunities and complementarities for the use of nano or micro bioactive glasses in the biomedical field.

1. Introduction

Hench invented bioactive glasses [1-3] in the Na2O-CaO-P2O5-SiO2 system, their utility has been widely proven in the area of bone restoration. Synthetic biomaterials are a good option for replacing biological bone grafts. Bioactive glasses, calcium phosphate and calcium carbonate are examples of synthetic materials used as biomaterials in orthopaedic surgery. They have the advantage of avoiding troubles linked to disease transmission. Thus, they are available in unlimited quantity, and they can be fitted for any person contrary to heterografts and xenografts. Precise studies to evaluate the biocompatibility and the physicochemical properties are required before the introduction of new synthetic materials for use in the biotechnological field. This work is focused on bioactive glasses. These glasses are particularly interesting due to their capacity to form a carbonated hydroxyapatite layer (HA) Ca10(PO4)6(OH)2. HA layer is very similar to the crystal composing the human bones.

Bioactive glasses may be synthesised using two different processes, both presenting advantages. The first is the synthesis of glass by fusion, it is historically used in many works [4-8]. The second presents an alternative using the polycondensation of a silica network via a so-called sol-gel synthesis [9-14].

This study is focused on the system CaO-P2O5-SiO2 which have shown some potential in their properties on biomedical field [15-17]. The synthesis and characterization of two bioactive glasses will be developed using the two different methods mentioned earlier. The development will focus on the effect of bioactive particles size on the kinetic of bioactivity.

In this study, nano-sized and micro-sized bioactive particles in the system CaO-P2O5-SiO2 were synthesized. Their chemical composition, microstructure, and bioactivity were investigated. Obtained results allow for a wider range of applications, particularly
in the field of biotechnology including but not limited to bone restoration,
bones regrowth, anti-bacteriological or metallic prothesis coating.

2. Materials and methods

2.1 Glass synthesis

2.1.1 Micro bioactive *glass (BG) synthesis process*. Preparation of the bioactive glass (46S6) by melting was previously described in our works [18]. The 46S6 synthesized in this study is a quaternary glass with the following molar percentage composition: 46 SiO2, 24 CaO, and 6 P2O5 and 24 Na2O. The melting process for the elaboration of the bioactive glass use silicon oxide (SiO2), Sodium metasilicate (Na2SiO3), Sodium metaphosphate (Na3P3O9), Calcium metasilicate (CaSiO3). These elements were weighed then mixed in a polyethene container for 2 hours in a planetary mixer. Origin and purity of these chemicals can be seen in table 1.

Table 1. Origin and purity of products for the melting process.

Chemical Name	Source	Mole fraction purity [a]
Silicon oxide (SiO_2)	Sigma-Aldrich Chemistry	0.9980
Sodium metasilicate (Na_2SiO_3)	Fisher chemical	≥ 0.97
Sodium metaphosphate ($Na_3P_3O_9$)	Alfa Aesar	0.95
Calcium metasilicate ($CaSiO_3$)	Alfa Aesar	≥ 0.97

[a] Purity of these elements has been controlled but has not been purified again.

Premixed materials were melted in a platinum crucible placed in an electric furnace. The first rise of temperature rate was 10 °C min-1 from 20 °C to 900 °C for a duration of 1 hour to decarbonate all products previously prepared, it is the calcination phase. After this first step, a new rise of temperature at 20 °C min-1 was conducted. The temperature was stabilized to 1350 °C for 3 additional hours, it is the melting phase. The thermal elaboration process is described in figure 1. After this 3-hour period of melting, the sample was air quenched and transferred to a preheated brass mould. The last step, the glass has been annealed at Tg ± 20 K (540 °C for 46S6) for 4 hours to stabilize the glass and to reduce physical tensions due to a brutal decrease in temperature during quenching. After this thermic treatment, the glass will be crushed to micrometres then subdued through a sieve to recover 60 ± 15 µm glass powder.

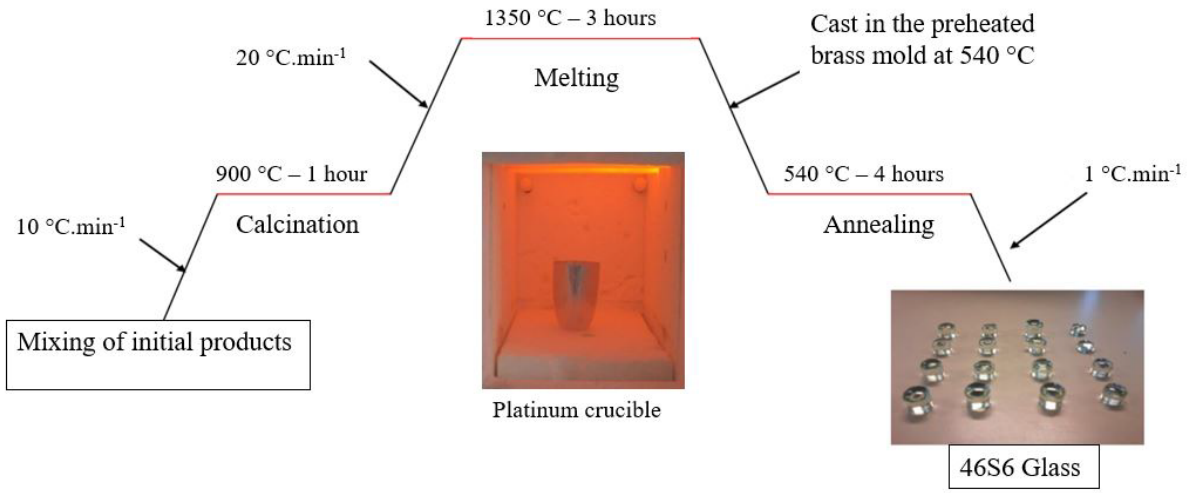

Figure 1. Thermal elaboration process for melting-made glass.

2.1.2 Nano bioactive *glass (NBG) synthesis process.* The nano bioactive glass (NBG) synthesized in this study is a ternary NBG with the following molar percentage composition: 55 SiO_2, 40 CaO, and 5 P_2O_5. The material was prepared from tetraethyl orthosilicate (TEOS), sodium trimetaphosphate ($Na_3P_3O_9$), calcium nitrate tetrahydrate ($Ca(NO_3)_2$ $4H_2O$) and ammonia (NH_3 H_2O). Furthermore, Octanol, Triton® X-100, and cyclohexane were also used as a surfactant and oil phase to prepare the emulsion. In this water in oil emulsion, the aqueous phase is dispersed to form microdroplets protect by a monolayer of surfactant molecules. The origin and purity of the product can be seen in table 2.

Table 2. Origin and purity of products for the sol-gel process.

Chemical Name	Source	Mole fraction purity [a]
Tetraethyl Orthosilicate (TEOS: $SiC_8H_{20}O_4$)	Merck	0.98
Sodium trimetaphosphate ($Na_3P_3O_9$)	Alfa Aesar	≥ 0.95
Calcium nitrate tetrahydrate ($Ca_2N_2O_6$ $4H_2O$)	Merck	0.99
Ammonia (NH_3 H_2O)	Carlo Erba Reagents	≥ 0.95
Octanol	Alfa Aesar	0.99
Triton® X100	Alfa Aesar	0.99
Cyclohexane	Fisher Chemical	≥ 0.95

[a] Purity of these elements has been controlled but has not been purified again

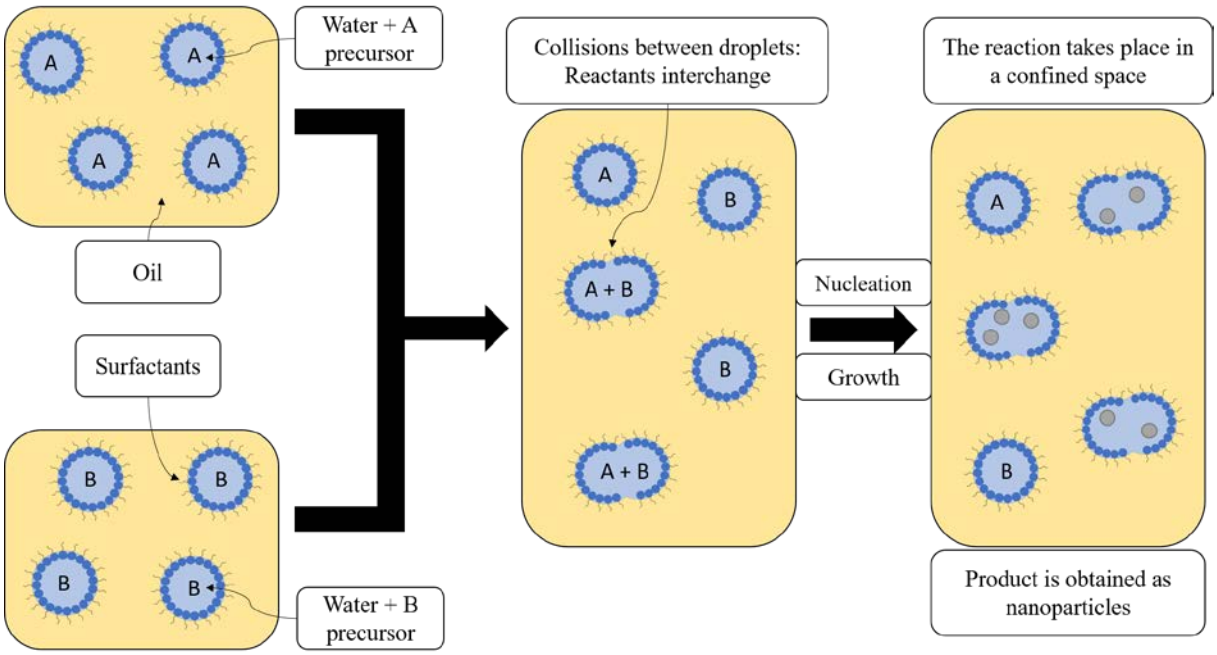

Figure 2. Diagram of the synthesis system for emulsion.

This process is based on the preparation and mixing of two different emulsions A and B.
Emulsion A is an aqueous ammonia phase containing TEOS and sodium trimetaphosphate. To this emulsion will be added the two surfactants (Triton® X-100 and octanol) and the oil phase (cyclohexane). This mixture will remain strongly stirred for one hour to allow the hydrolyzation of TEOS and sodium trimetaphosphate. Emulsion B is an aqueous phase based on calcium nitrate tetrahydrate, to which will also be added the same two surfactants and cyclohexane. This synthesis system is presented in a diagram in figure 2. Both emulsion compositions are resumed in table 3.

Table 3. Composition of each emulsions.

	Emulsion A	Emulsion B
Aqueous phase	Ammonia, water	Calcium nitrate tetrahydrate, water
Surfactants	Triton® X-100, Octanol	Triton® X-100, Octanol
Oil phase	Cyclohexane	Cyclohexane

After their separated preparation, the two emulsions were mixed together for a duration of 1 hour under a constant and vigorous speed then stirring have been stopped and the preparation let to rest for 45 minutes.
After this growing time, a white product was collected by centrifugal (6000 g) and washed repeatedly with ethanol to eliminate the most surfactant. Finally, drying to solid at 100 °C for 4 h and calcinated at 620 °C for 4 h to eliminate all surfactant trace.

2.2 Physicochemical characterization techniques

2.2.1 Size and *specific area measurement.* The determination of the size distribution of the synthesized nano particles was obtained using Dynamic Light Scattering (DLS) through Zetasier (Nano ZS, Malvern). This technique was used to measure the hydrodynamic diameter of the nanoparticles from 1 nm to 10 µm with ± 0.4 nm using the diffraction of light. Theses hydrodynamic measurements were performed at a 90 ° angle, after the dilution of the sample (50 µg mL^{-1}) in a saline solution to maintain

Brownian motion. The particles were dispersed in the saline solution for 15 min in an ultrasound bath to disperse possibly-formed agglomerates.
The specific surface area was calculated by the Brunauer-Emmett-Teller (BET) N_2 adsorption-desorption method (Flowsorb II 2300, Coultronics France SA), the total pore volume and the average pore diameter are also determined.

2.2.2 Thermal analysis. Thermal characteristics of the elaborated glasses (nano and micro) have been measured by using Differential Scanning Calorimetry (DSC). Measurements of thermal characteristics were carried out by means of a Setaram Labsys 1600TG-DTA/DSC thermal analyser under N_2 gas atmosphere at 0.1 MPa without pressure control. This analyser has been calibrated using a 3-peak calibration with $SrCO_3$, $BaCO_3$, and K_2CrO_4. First experimentation has been made using the same platinum crucible of 100 µL as the one used for all the analyses to eliminate the effect of the crucible in results. The microbalance sensitivity of the thermogravimetric simultaneous thermal analyser is better than 0.1 µg and its temperature precision is ± 1 K. DSC signal is used in this work. Bioactive glasses were studied at a heating rate of 5 °C min^{-1} raised from room temperature (around 20-25 °C) to 1350 °C. Each time, 40 ± 0.1 mg of glass powder was heated in a platinum crucible and at the same time, another empty platinum crucible was used as control (differential measurement).

2.2.3 Structure and functional groupings in elaborated materials. X-ray Diffraction (XRD) and Fourier transformed Infra-Red spectroscopy (FT-IR) have been used to control physicochemical properties of elaborated glasses. The control of the amorphous nature and the potential formation of new functional groups in these compounds were the main objectives of this characterization.
XRD patterns were recorded between 5 and 90 ° (2θ) by a PANalytical X'Pert PRO diffractometer with a precision of 0.026 ° by steps and a count time of 40 s per step using Cu Kα. Voltage was of 50 kV and the current was 40 mA during analyses. Powdered samples were prepared for XRD analysis and back-loaded into steel sample holders.
For FT-IR analysis, samples were embedded in KBr pellets and recorded by Bruker Equinox 55 spectrometer between 4000 cm^{-1} and 400 cm^{-1} in transmittance mode with a resolution of 2 cm^{-1}. FT-IR and XRD analyses were carried out at ambient temperature.

2.3 Soaking preparation for in vitro chemical reactivity for bioactive glasses
The in vitro bioactivity was evaluated by the immersion of 30 mg of nanopowder and 30 mg of micropowder in 60 ml of SBF [19] in the same conditions. The chemical composition of SBF is presented in table 4 and similar to the chemical composition of human blood plasma. These tests have been carried out for different duration of soaking composed by short (2, 4, 8, 16 h, 1, 3 days) or long delay (2 weeks, 1, and 2 months) and maintained at 37 °C under constant stirring. After soaking, samples have been removed from the SBF solution, rinsed with water and ethanol and dried at 75 °C for 3 h. The structure of each sample was analysed by XRD.

Table 4. Ionic composition of SBF compare to human blood plasma.

Ions (mM)	Na^+	K^+	Mg_2^+	Ca_2^+	Cl^-	HCO_3^-	HPO_4^{2-}	SO_4^{2-}
SBF	142.0	5.0	1.5	2.5	147.8	4.2	1.0	0.5
Plasma	142.0	5.0	1.5	2.5	103.0	27.0	1.0	0.5

Experimental concentration uncertainties u(C) = ± 0.1 mM.

2.4 Cytotoxicity tests

Cytotoxicity tests have been made for both glasses. The cytotoxicity of the micrometric glass has been studied and described in further research [20]. Due to the unknown harmfulness of nanoparticle powder, these tests have been made in a diluted solution of tween 20® added to a solution of Dulbecco's Modified Eagles Medium (DMEM). The DMEM is a solution used for the supply of nutrients necessary for the maintenance and proliferation of different types of cells in vitro. Cytotoxicity tests have been made for two different cell line: SaOs-2 (osteoblastic) and EA.hy926 (endothelial), two durations: 3 and 24 hours and three different concentration of nanoparticles: 25, 10, 1 µg/mL [21].

2.5 Statistical analysis.
For all the tests, data are expressed as the mean ± SD of three independent experiments.

3. Results and discussion

3.1 Physicochemical characterization of glasses

3.1.1 Size and specific area of melting and sol-gel bioactive glasses. Dynamic light scattering results show spherical particles with medium size around 110 nm for the sol-gel-made glass as shown in figure 3.

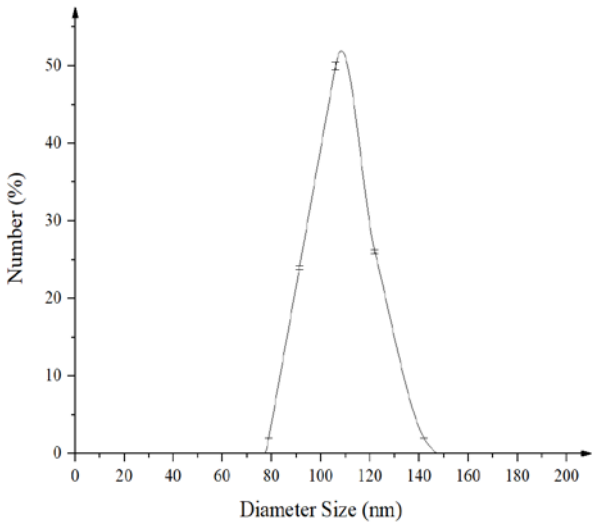

Figure 3. Size distribution of the nano bioactive glass using DLS.

The size of the glass particles synthesized by melting is ensured using sieves allowing the sizes to pass less than 40 µm and preventing the passage of sizes greater than 63 µm it results most of the particles are around 60 µm. BET obtained result show that the surface area decreases in function of particles size, from 69.4 to 1.1 $m^2 g^{-1}$. These results can be seen in table 5

Table 5. Surface area, pore volume and pore diameter of studied glasses.

Glass size	Surface area ($m^2 g^{-1}$)[a]	Pore volume ($cm^3 g^{-1}$)[b]	Pore diameter (Å)[c]
110 nm	69.4	0.131	72.08
60 µm	1.1	0.001	33.16

[a] Experimental surface area uncertainty u(sa) = 0.1 m^2 g^{-1}.
[b] Experimental pore volume uncertainty u(pv) = 0.01 cm^3 g^{-1}.
[c] Experimental pore diameter uncertainty u(pd) = 0.01 Å.

A higher specific surface area enables a faster ion release for bioactive materials. This rise in ion release and ions transfer allow the possibility to obtain high healing kinetic for biomaterials.

3.1.2 Thermal *analysis results of studied bioactive glasses.* Each DSC spectra show the presence of a glass transition temperature, a crystallisation temperature and a melting temperature respectively called as Tg, Tc and Tf. According to literature [22], each synthetized material may be a glass. DSC spectra of materials are presented in figure 4 and 5.

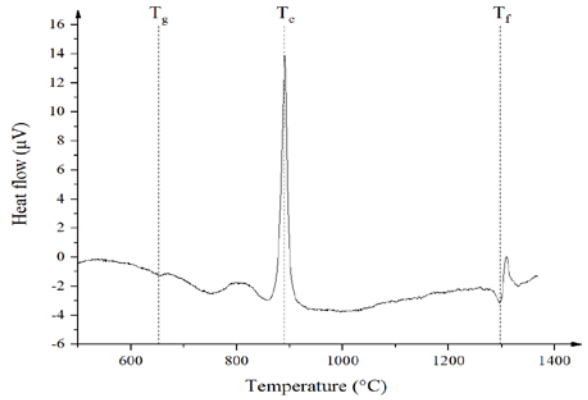

Figure 4. DSC of the sol-gel-made nano glass.

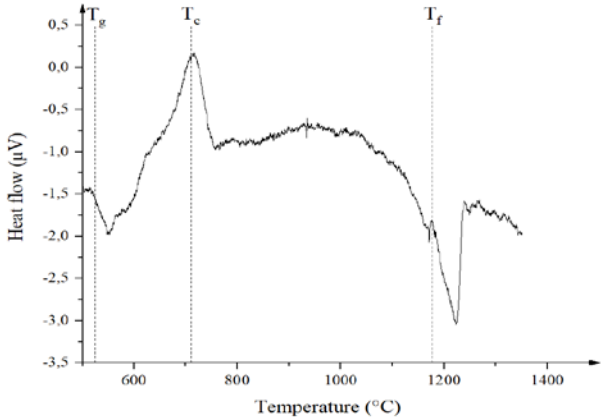

Figure 5. DSC of the melting-made micro glass.

3.1.3 Structure *and functional grouping of bioactives glasses after soaking*. FTIR results shown similar results for both glasses. The vibration strips at 470 cm^{-1} and 1200 cm^{-1} correspond to characteristic Si-O-Si bonds. While the vibration strips at 1400 cm^{-1}, 1070 cm^{-1}, 925 cm^{-1} and 567 cm^{-1} correspond to the phosphate and carbonate groups. These results are shown in figure 6.

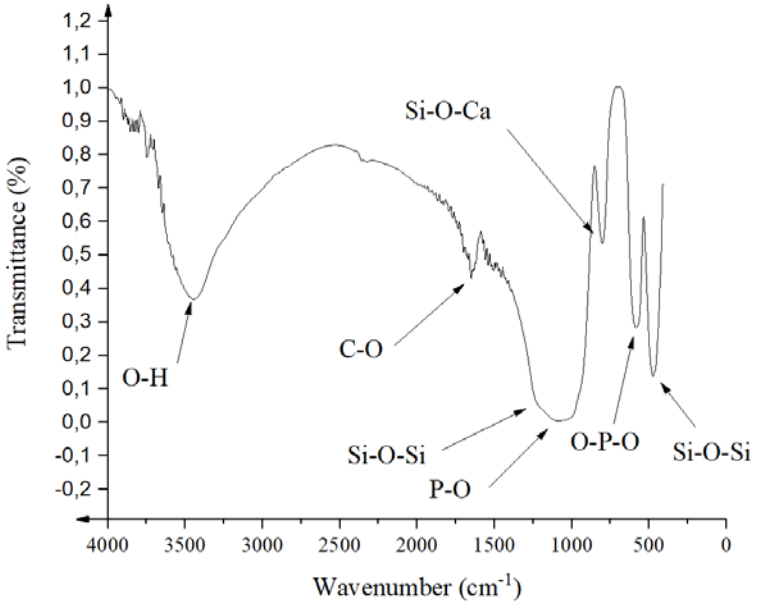

Figure 6. FTIR results of soaked glasses.

The XRD diffractogram of the micrometric material showed at figure 7 presents no sign of crystallisation before immersion. This diffractogram determine the micromaterial as glass. Results show a crystallisation of the glass into a similar form as the HA (use here as reference). The obtained results presented in this work show the first diffractograms with a crystallization effect. In the case of micrometric glass, it has been found that it is recognizable from the second week.

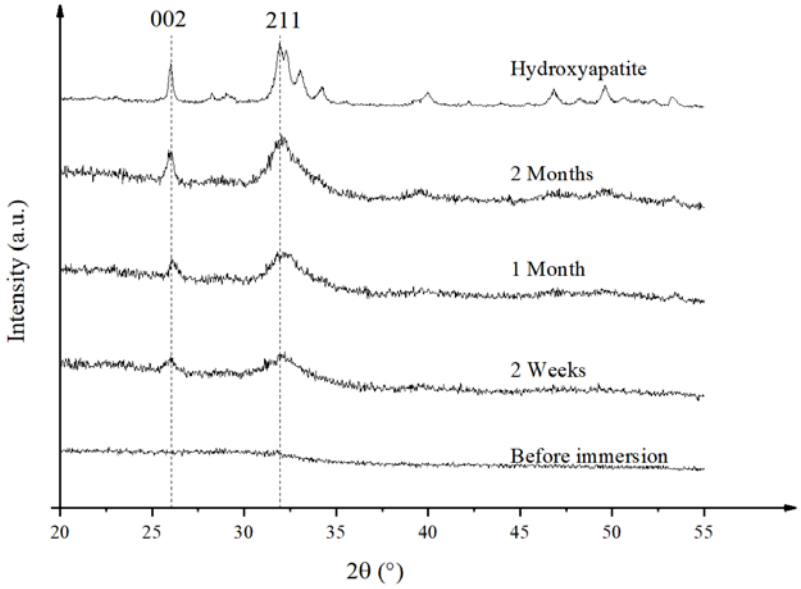

Figure 7. XRD diffractogram of melting-made micro glass before and after soaking.

The XRD diffractogram of the nanometric material showed at figure 8 doesn't presents sign of crystallisation before immersion. This diffractogram determine the nanomaterial as glass. Results show a crystallisation of the glass into a similar form as the HA. In the case of nanometric glass, it has been found that it is recognizable from the eighth hour.
The comparison between the two diffractograms allow to link the size of the bioactive particle with the specific surface area and the kinetic of crystallisation. In this case, the kinetics of crystallization is 4 times faster in the case of nanoscale bioactive glass when in that of micrometric glass whereas a factor of 70 separates their specific surface.

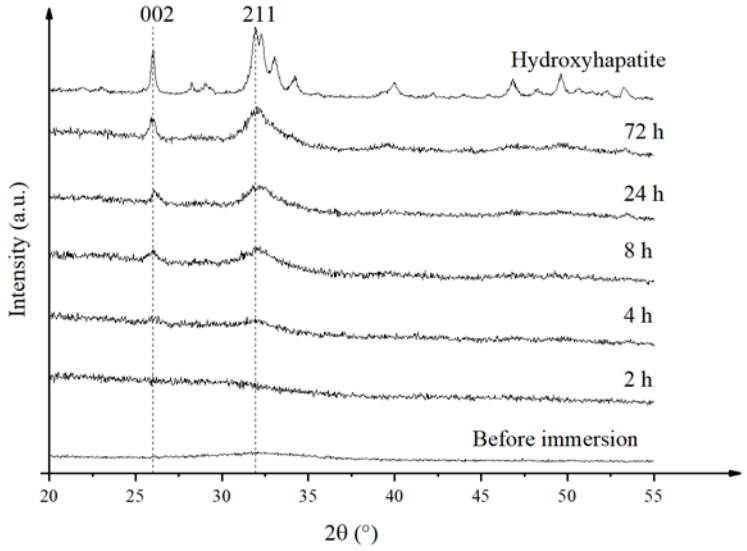

Figure 8. XRD diffractogram of sol-gel-made nano glass before and after soaking.

3.2 Cytotoxicity tests results

The cytotoxicity tests presented in figure 9 show that nanometric glass (110 nm) is relatively well tolerated by cells. These concentrations therefore have no toxicity for the cells studied. Nevertheless, the nanometric particles exhibit a phenomenon of aggregation once immersed in tween 20. The results therefore have great variation and are very difficult to reproduce as shown by the variations shown in the figure.

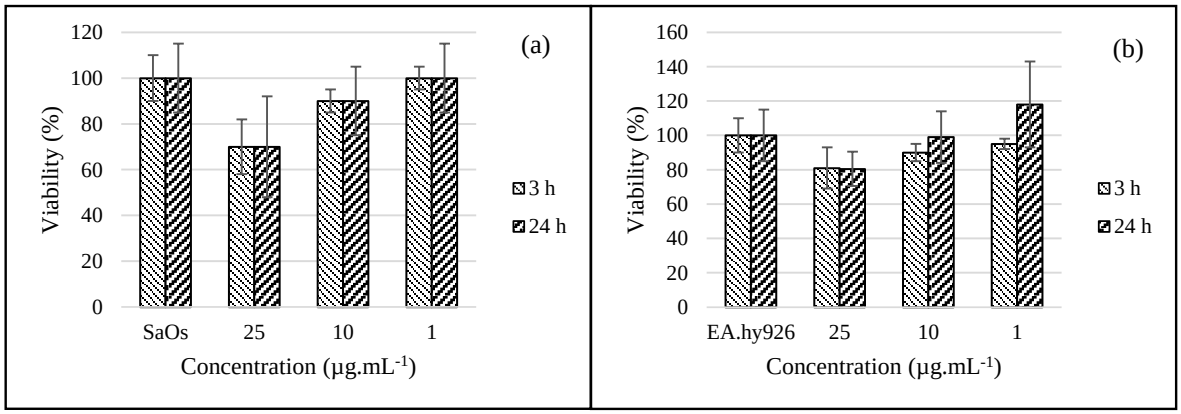

Figure 9. Viability of SaOs-2 (a) and EA.hy926 (b) cell lines as a function of nanoparticle concentration.

4. Conclusion

Despite major differences in the synthesis of the two materials presented in this article, the physicochemical characterization shows that they are bioactive glasses. Their characterisation highlights their amorphous nature and their capacity to form chemical bond and turn into crystal.

This study shows that changing the size of biomaterials causes changes in its specific surface area, pore size and ion exchanges capacity with its environment. In our case the reduction of a size ratio of 545 increases the specific surface area from 1.1 to 69.4 m^2 g^{-1} and makes it possible to obtain a crystallization similar to 2 weeks of immersion in 3 days of immersion only for the case of nano bioactive glass of 110 nm.

Nevertheless, it is important to highlight other differences that may affect the kinetics of bioactivity of the glasses studied during this research. Indeed, the composition, therefore the chemical environment of the vitreous matrix plays an important role in the ion exchanges between the medium (here SBF) and the surface of the glass. Consequently, glasses properties and particularly their composition may lead to the change on the kinetic of bioactivity.

In the end, the comprehension of all the elements and more particularly of the interactions of these elements between them is very important. Accurate knowledge will allow the development of biomaterials, effective, adaptable depending on the nature of the lesion undergone, its location and the constitution of the patient. With the aim of deepening the interaction of the size of the bioactive glass nanotubes and the kinetics of bioactivity, a study has been initiated and in progress to have more data to yield significant statistics.

5. References

[1] Hench LL, Splinter RJ, Allen WC and Greenlee TK, 1971 *J. Biomed. Mater. Res.* **5** 117
[2] Hench LL, 1998 *Biomaterials* **19** 1419
[3] Hench LL, 2002 *Science* **295** 1014
[4] Wers E, Oudadesse H, Lefeuvre B, Bureau B and Merdrignac-Conanec O, 2014 *Thermochimica Acta* **580** 79

[5] Wers E, Oudadesse H, Lefeuvre B, Lucas-Girot A, Rocherullé J and Lebullenger R 2014 *Journal of Thermal Analysis and Calorimetry* **117** 579
[6] Wers E, Oudadesse H, Lefeuvre B, Merdrignac-Conanec O and Barroug A 2015 *Applied Surface Science* **353** 200
[7] Franchini M, Lusvardi G, Malavasi G and Menabue L 2012 *Materials Science and Engineering: C* **32** 1401
[8] Dietrich E, Oudadesse H, Lucas-Girot A, Le Gal Y, Jeanne S and Cathelineau G 2008 *Applied Surface Science* **255** 391
[9] Zheng K and Boccaccini AR 2017 *Advances in Colloid and Interface Science* **249** 363
[10] Hench LL and West JK 1990 *Chemical Reviews* **90** 33
[11] Itoh H and Sugimoto T 2003 *Journal of Colloid and Interface Science* **265** 283
[12] Lukowiak A, Lao J, Lacroix J and Nedelec JM. 2013 *Chemical Communications* **49** 6620
[13] Nabian N, Jahanshahi M and Rabiee SM 2011 *Journal of Molecular Structure* **998** 37
[14] Saboori A, Rabiee M, Moztarzadeh F, Sheikhi M, Tahriri M and Karimi M 2009 *Materials Science and Engineering: C* **29** 335
[15] Hench L.L 1997 *Solid State Mater. Sci.* ***2***, 604
[16] Itoh H and Sugimoto T 2003 *J. Colloid Interface Sci.* **265** 283
[17] Hench LL 2000 *Key Eng. Mater.* **192–195** 575
[18] Rocton N, Oudadesse H and Lefeuvre B 2018 *Thermochimica Acta* **668** 58
[19] Kokubo T, Kushitani H, Ohtsuki C, Sakka S and Yamamuro T 1992 *Journal of Materials Science: Materials in Medicine* **3** 79
[20] Oudadesse H, Dietrich E, Bui, XV, Le Gal Y, Pellen P and Cathelineau G 2011 *Applied Surface Science* **257** 8587
[21] Pellen-Mussi P, Tricot-Doleux S, Neaime C, Nerambourg N, Cabello-Hurtado F, Cordier S, Grasset F and Jeanne S *Journal of Nanoscience and Nanotechnology* 2018 3148
[22] J Zarzycki, *Les verres et l'état vitreux*, 1st ed., Masson, Paris, 1982.